

Symmetric lens with extended depth of focus

Sung Nae Cho*

*MEMS & Packaging Group, Samsung Advanced Institute of Technology,
Mt. 14-1 Nongseo-dong Giheung-gu, Yongin-si Gyeonggi-do, 446-712, South Korea
(Dated: Prepared 17 July 2008)*

The lens surface profile is derived based on the instantaneous focal length versus the lens radius data. The lens design based on instantaneous focal length versus the lens radius data has many useful applications in software assisted image focusing technology.

I. INTRODUCTION

The software assisted image focusing is an emerging technology which is expected to replace the traditional methods of autofocus in image manipulation devices, such as digital cameras and mobile phones. Unlike the traditional methods, where the focusing of images is done by mechanically movable parts, the software assisted technology produces focused images by processing it through specialized image reconstruction algorithm. The transition from mechanical to software assisted image focusing can be attributed to the (1) demand for thinner and lighter products by customers, and (2) the advancements in manufacturing process for faster and more power efficient digital signal processors. With autofocus by mechanically movable parts, the demand for thinner and lighter products is becoming a top hurdle for manufacturing process. On the other hand, the advancements in more power efficient and faster digital signal processors make software assisted image focusing technology ideal for satisfying customer's demand for thinner and lighter image developing products such as digital cameras and mobile phones to name a few.

At the heart of software assisted image autofocus technology is the specialized image reconstruction algorithm permanently coded into the built in digital signal processor. The actual layout of the code base for image reconstruction algorithm varies among different manufacturers and many manufacturers do not disclose their algorithms to public as they constitute a trade secret. The image reconstruction algorithm can be codified based on instantaneous focal length versus the lens radius data(**author?**) [1]. Once this specialized image reconstruction algorithm is adopted for the system, a lens must be designed so that its output matches the instantaneous focal length versus the lens radius data, which information was assumed and used as input to the image reconstruction code base.

In this work, a formula for the lens surface profile is presented. The derivation of lens surface profile is solely based on the instantaneous focal length versus the lens radius data; and therefore, the result is expected to find useful applications in software assisted image focusing

technologies.

II. INSTANTANEOUS FOCAL LENGTH DATA

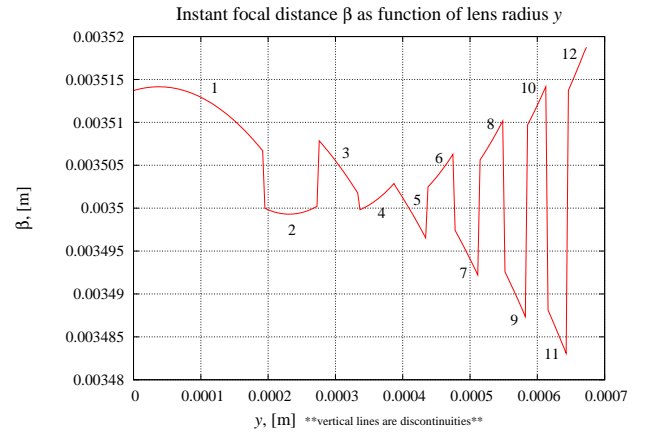


Figure 1: Instantaneous focal length versus the lens radius, where both are measured in meters. The normal incidence is assumed for the incoming light rays.

Alexander and Lukyanov have recently filed for a patent which deals with image reconstruction algorithm with applications in software assisted image focusing technology. In their proposal, they claim to have obtained an optimal image processing solution, which is expected to be a significant improvement over the predecessor(**author?**) [2]. Behind their optimization is the instantaneous focal length versus the lens radius data illustrated in Fig. 1, which result assumes a normal incidence for the incident light waves. In the figure, β denotes the instantaneous focal length and y is the lens radius. Each of the twelve segmented curves can be represented by the quadratic polynomial

$$\beta_i(y) = a_i y^2 + b_i y + c_i, \quad (1)$$

with coefficients (a_i, b_i, c_i) given by

$$a_1 = -313.07, \quad b_1 = 0.0235, \quad c_1 = 0.0035137034,$$

$$a_2 = 534.53, \quad b_2 = -0.2472, \quad c_2 = 0.003527877626,$$

$$a_3 = -309.02, \quad b_3 = 0.0818, \quad c_3 = 0.0035088062,$$

*Electronic address: sungnae.cho@samsung.com

$$a_4 = 536.05, b_4 = -0.3275, c_4 = 0.0035493232,$$

$$a_5 = -306.12, b_5 = 0.1182, c_5 = 0.003502912672,$$

$$a_6 = 539.03, b_6 = -0.3891, c_6 = 0.003569538239,$$

$$a_7 = -303.68, b_7 = 0.1463, c_7 = 0.003496845208,$$

$$a_8 = 542.21, b_8 = -0.4417, c_8 = 0.003589312176,$$

$$a_9 = -301.27, b_9 = 0.1695, c_9 = 0.00349080193,$$

$$a_{10} = 545.96, b_{10} = -0.4895, c_{10} = 0.003609151039,$$

$$a_{11} = -298.81, b_{11} = 0.1893, c_{11} = 0.003484870978,$$

$$a_{12} = 179.08, b_{12} = -0.0474, c_{12} = 0.003469596542,$$

where the subscript i denotes the i th curved segment in Fig. 1. The curve fitting was done by linear regression. The physical lens, whose output satisfies the instantaneous focal length versus the lens radius data defined in Fig. 1, is one of the variants of lens with extended depth of focus (author?) [3, 4, 5]. With Eq. (1), I shall solve for the lens surface profile whose output matches the instantaneous focal length versus the lens radius data defined in Fig. 1.

III. THE LENS SURFACE EQUATION

A. Derivation

When a ray of light passes across media of different refractive indices, its path is governed by the Snell's law,

$$n_\phi \sin \phi = n_\theta \sin \theta, \quad (2)$$

as illustrated in Fig. 2. Here, $n_\phi \equiv n_\phi(\omega)$ and $n_\theta \equiv n_\theta(\omega)$ are frequency dependent refractive indices with ω denoting the angular frequency of the light. The parameters ϕ and θ represent the angle of incidence and angle of refraction, respectively.

If \mathbf{N} denotes the normal vector to the local point $y = \gamma$ on the curve $x = h(y)$, then it can be shown

$$\|-\mathbf{N} \times (-\mathbf{e}_1)\| = \|\mathbf{N}\| \|\mathbf{e}_1\| \sin \phi = N \sin \phi$$

and the expression for $\sin \phi$ becomes

$$\sin \phi = \frac{\|\mathbf{N} \times \mathbf{e}_1\|}{N}, \quad N \equiv \|\mathbf{N}\|, \quad (3)$$

where \mathbf{e}_1 is the unit basis for the x axis.

Similarly, the expression for $\sin \theta$ may be obtained by considering vectors \mathbf{A} , \mathbf{B} , and \mathbf{C} of Fig. 2. The vectors \mathbf{A} , \mathbf{B} , and \mathbf{C} satisfy the relation,

$$\mathbf{A} + \mathbf{B} = \mathbf{C}. \quad (4)$$

In explicit form, vectors \mathbf{A} and \mathbf{B} are defined as

$$\mathbf{A} = -\gamma \mathbf{e}_2, \quad \mathbf{B} = (\beta - \alpha) \mathbf{e}_1, \quad (5)$$

where \mathbf{e}_2 is the unit basis for the y axis. With Eqs. (4) and (5), the vector \mathbf{C} becomes

$$\mathbf{C} = (\beta - \alpha) \mathbf{e}_1 - \gamma \mathbf{e}_2. \quad (6)$$

The vector cross product $\mathbf{N} \times \mathbf{C}$ is given by

$$\mathbf{N} \times \mathbf{C} = (\beta - \alpha) \mathbf{N} \times \mathbf{e}_1 - \gamma \mathbf{N} \times \mathbf{e}_2$$

and its magnitude becomes

$$\|\mathbf{N} \times \mathbf{C}\| = \|(\beta - \alpha) \mathbf{N} \times \mathbf{e}_1 - \gamma \mathbf{N} \times \mathbf{e}_2\| = NC \sin \theta, \quad (7)$$

where $N \equiv \|\mathbf{N}\|$ and $C = \|\mathbf{C}\|$. Utilizing Eq. (6), C may be expressed as

$$C = (\mathbf{C} \cdot \mathbf{C})^{1/2} = [(\beta - \alpha)^2 + \gamma^2]^{1/2}$$

and the Eq. (7) is solved for $\sin \theta$ to yield

$$\sin \theta = \frac{\|(\beta - \alpha) \mathbf{N} \times \mathbf{e}_1 - \gamma \mathbf{N} \times \mathbf{e}_2\|}{N [(\beta - \alpha)^2 + \gamma^2]^{1/2}}. \quad (8)$$

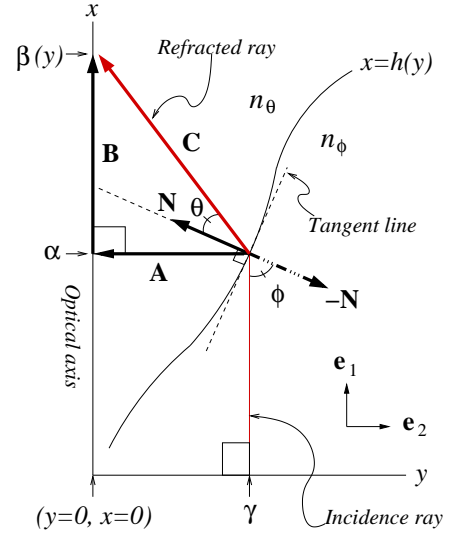


Figure 2: Illustration of Snell's law.

Insertion of Eqs. (3) and (8) into the Snell's law of Eq. (2) gives

$$\frac{n_\phi}{n_\theta} = \frac{\|(\beta - \alpha) \mathbf{N} \times \mathbf{e}_1 - \gamma \mathbf{N} \times \mathbf{e}_2\|}{\|\mathbf{N} \times \mathbf{e}_1\| [(\beta - \alpha)^2 + \gamma^2]^{1/2}}. \quad (9)$$

By definition, the normal vector \mathbf{N} satisfies the relation,

$$g(x, y) = x - h(y),$$

where $g(x, y)$ is a function whose gradient gives \mathbf{N} ,

$$\mathbf{N} = \nabla g = \frac{\partial g}{\partial x} \mathbf{e}_1 + \frac{\partial g}{\partial y} \mathbf{e}_2 = \mathbf{e}_1 - \frac{\partial h}{\partial y} \mathbf{e}_2.$$

Because \mathbf{N} is the normal vector at the location $(x = \alpha, y = \gamma)$, I write

$$\mathbf{N} = \mathbf{e}_1 - \left. \frac{\partial h}{\partial y} \right|_{y=\gamma} \mathbf{e}_2. \quad (10)$$

The following vector cross products are valid,

$$\begin{aligned} \mathbf{N} \times \mathbf{e}_1 &= \mathbf{e}_1 \times \mathbf{e}_1 - \left. \frac{\partial h}{\partial y} \right|_{y=\gamma} \mathbf{e}_2 \times \mathbf{e}_1, \\ \mathbf{N} \times \mathbf{e}_2 &= \mathbf{e}_1 \times \mathbf{e}_2 - \left. \frac{\partial h}{\partial y} \right|_{y=\gamma} \mathbf{e}_2 \times \mathbf{e}_2, \end{aligned}$$

where Eq. (10) was used to replace \mathbf{N} . Since $\mathbf{e}_1 \times \mathbf{e}_1 = \mathbf{e}_2 \times \mathbf{e}_2 = 0$, the previous relations reduce to

$$\mathbf{N} \times \mathbf{e}_1 = \left. \frac{\partial h}{\partial y} \right|_{y=\gamma} \mathbf{e}_3, \quad \mathbf{N} \times \mathbf{e}_2 = \mathbf{e}_3, \quad (11)$$

where \mathbf{e}_3 is the unit basis for the z axis of which satisfies the relation,

$$\mathbf{e}_1 \times \mathbf{e}_2 = \mathbf{e}_3, \quad \mathbf{e}_2 \times \mathbf{e}_1 = -\mathbf{e}_3.$$

Insertion of Eq. (11) into Eq. (9) gives

$$\frac{n_\phi}{n_\theta} = \frac{(\beta - \alpha) \left. \frac{\partial h}{\partial y} \right|_{y=\gamma} - \gamma}{\left. \frac{\partial h}{\partial y} \right|_{y=\gamma} [(\beta - \alpha)^2 + \gamma^2]^{1/2}},$$

which expression can be rearranged to yield

$$\left. \frac{\partial h}{\partial y} \right|_{y=\gamma} = \frac{\gamma}{\beta - \alpha - \frac{n_\phi}{n_\theta} [(\beta - \alpha)^2 + \gamma^2]^{1/2}}, \quad (12)$$

where α and γ are constants of which are depicted in Fig. 2.

For Alexander and Lukyanov's optical element, the instantaneous focal function $\beta \equiv \beta(y)$ in Eq. (12) is as defined in Fig. 1. The γ for the y axis is not anything special, of course. Any y belonging to the domain of h satisfies the Eq. (12). The generalization of Eq. (12) for all y belonging to the domain of h is done by making the following replacements:

$$\alpha \rightarrow x, \quad \gamma \rightarrow y, \quad \left. \frac{\partial h}{\partial y} \right|_{y=\gamma} \rightarrow \frac{\partial h}{\partial y} = \frac{dx}{dy}.$$

With these replacements, Eq. (12) gets re-expressed in form as

$$\frac{dx}{dy} = \frac{y}{\beta - x - \frac{n_\phi}{n_\theta} [(\beta - x)^2 + y^2]^{1/2}}. \quad (13)$$

How is the instantaneous focal function, β , restricted? The β in Eq. (13) is restricted so that the expression for dx/dy does not blow up. Equation (13) is well behaved if and only if the denominator satisfies the condition,

$$\beta - x - \frac{n_\phi}{n_\theta} [(\beta - x)^2 + y^2]^{1/2} \neq 0.$$

To solve for β , I shall first rearrange the previous expression to get

$$\beta - x \neq \frac{n_\phi}{n_\theta} [(\beta - x)^2 + y^2]^{1/2}.$$

Squaring both sides,

$$(\beta - x)^2 \neq \frac{n_\phi^2}{n_\theta^2} (\beta - x)^2 + \frac{n_\phi^2}{n_\theta^2} y^2,$$

and regrouping the terms, I find

$$(\beta - x)^2 \left(1 - \frac{n_\phi^2}{n_\theta^2} \right) \neq \frac{n_\phi^2}{n_\theta^2} y^2.$$

The resulting expression can be solved for β to yield

$$\beta \neq x \pm \frac{n_\phi y}{\sqrt{n_\theta^2 - n_\phi^2}}. \quad (14)$$

Equation (14) defines the restriction for the instantaneous focal function.

B. Lens surface profile

The profile of axially symmetric lens about its optical axis is obtained by solving the initial-value differential equation, Eq. (13),

$$\frac{dx}{dy} = \frac{y}{\beta - x - \frac{n_\phi}{n_\theta} [(\beta - x)^2 + y^2]^{1/2}}, \quad x(y_0) = x_0,$$

where $x(y_0) = x_0$ is the initial condition to be specified and the instantaneous focal function β satisfies the constrain defined in Eq. (14). Without loss of generality, one may choose $x(y = y_0 = 0) = 0$ for the initial condition and the lens profile satisfies the differential equation,

$$\frac{dx}{dy} = \frac{y}{\beta_i - x - \frac{n_\phi}{n_\theta} [(\beta_i - x)^2 + y^2]^{1/2}}, \quad (15)$$

$$x(0) = 0, \quad \beta_i \neq x \pm \frac{n_\phi y}{\sqrt{n_\theta^2 - n_\phi^2}},$$

where the index i in β_i comes from the fact that the input specification defined in Fig. 1 is piece wise continuous over range of x . The domain for each β_i is given by

$$\beta_1 : 0 \leq y \leq 0.00019182692,$$

$$\beta_2 : 0.00019519231 \leq y \leq 0.00027259615,$$

$$\beta_3 : 0.00027596154 \leq y \leq 0.00033317308,$$

$$\beta_4 : 0.00033653846 \leq y \leq 0.00038701923,$$

$$\beta_5 : 0.00039038462 \leq y \leq 0.00043413462,$$

$$\beta_6 : 0.0004375 \leq y \leq 0.00047451923,$$

$$\beta_7 : 0.00047788462 \leq y \leq 0.00051153846,$$

$$\beta_8 : 0.00051490385 \leq y \leq 0.00054855769,$$

$$\beta_9 : 0.00055192308 \leq y \leq 0.00058221154,$$

$$\beta_{10} : 0.00058557692 \leq y \leq 0.0006125,$$

$$\beta_{11} : 0.00061586538 \leq y \leq 0.00064278846,$$

$$\beta_{12} : 0.00064615385 \leq y \leq 0.00067307692.$$

The differential equation (15) has been solved using the Runge-Kutta method (author?) [6]. The Runge-Kutta routine has been coded in **FORTRAN 90** and the result for the case where $n_\phi = 1$ and $n_\theta = 1.5311$ is provided in Fig. 3. The physical lens may be obtained by revolving the curve about the x axis. Since the light ray is directed in the positive x direction, as illustrated in Fig. 4, it implies that the image sensor should be embedded inside the lens for the case where $n_\theta > n_\phi$.

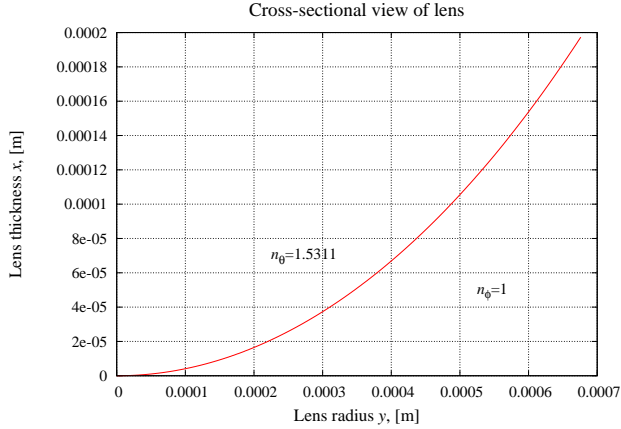


Figure 3: The lens cross-section, $n_\theta > n_\phi$.

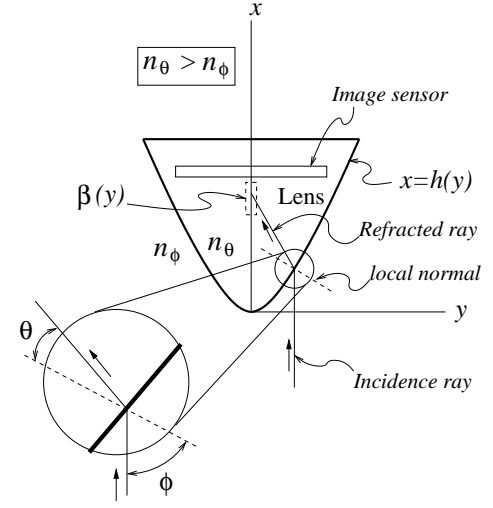


Figure 4: Location of the image sensor.

Reversing the values for two refractive indices, i.e., ($n_\phi = 1.5311$ and $n_\theta = 1$), the lens surface profile becomes as illustrated in Fig. 5. Again, the physical lens may be obtained by revolving the curve about the x axis. Since the light ray is directed in the positive x direction, the case $n_\theta < n_\phi$ represents the situation where light is exiting the lens medium. For this configuration, where $n_\theta < n_\phi$, the image sensor should be placed external to the lens medium, as illustrated in Fig. 6.

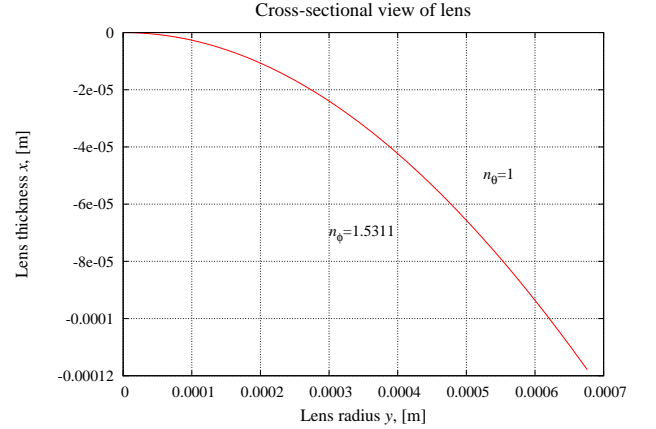


Figure 5: The lens cross-section, $n_\theta < n_\phi$.

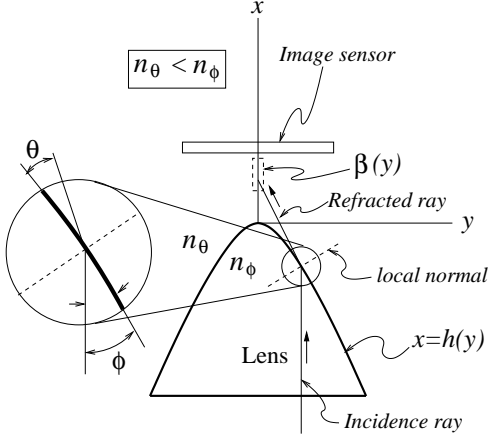


Figure 6: Location of the image sensor.

The plots of lens surface cross-section, Figs. 3 and 5, deceptively portray as if lens surface profile is represented by parabolic class of curves. To show graphically that this is not the case, the numerical data solutions obtained via Runge-Kutta method to graph Figs. 3 and 5 were linearly regressed to obtain

$$x_1 = a_1 y^6 + b_1 y^5 + c_1 y^4 + d_1 y^3 + e_1 y^2 + f_1 y + g_1, \quad (16)$$

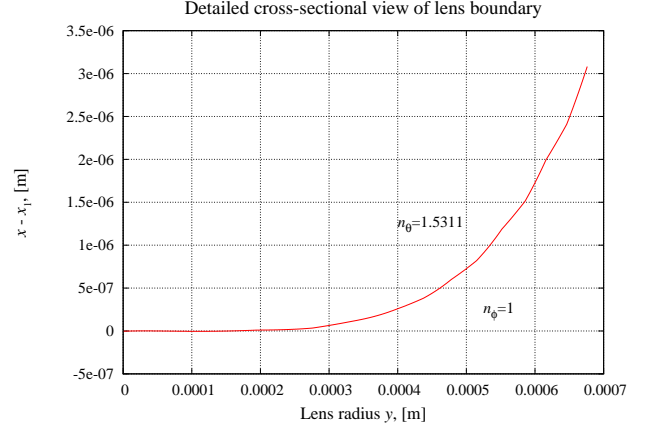
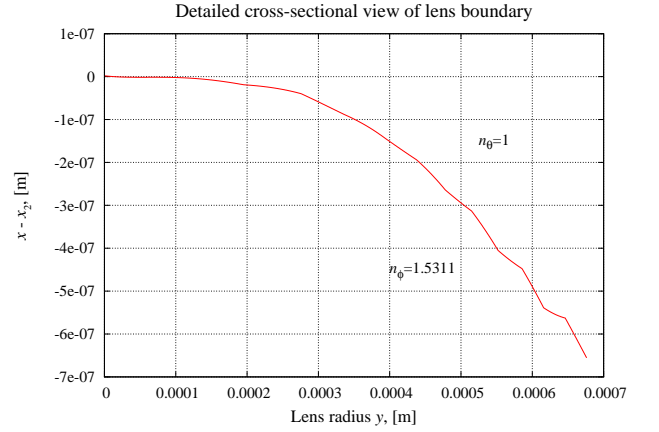
$$x_2 = a_2 y^6 + b_2 y^5 + c_2 y^4 + d_2 y^3 + e_2 y^2 + f_2 y + g_2, \quad (17)$$

where x_1 is the polynomial curve fit for Fig. 3, x_2 is the polynomial curve fit for Fig. 5, and the coefficients are given by

$$\begin{aligned} a_1 &= -8 \times 10^{13}, \quad b_1 = 2 \times 10^{11}, \quad c_1 = -1 \times 10^8, \\ d_1 &= 52523, \quad e_1 = 403.1, \quad f_1 = 3 \times 10^{-4}, \\ g_1 &= -3 \times 10^{-9}, \end{aligned}$$

$$\begin{aligned} a_2 &= 5 \times 10^{13}, \quad b_2 = -1 \times 10^{11}, \quad c_2 = 1 \times 10^8, \\ d_2 &= -29916, \quad e_2 = -264, \quad f_2 = -2 \times 10^{-4}, \\ g_2 &= 2 \times 10^{-9}. \end{aligned}$$

If x_1 represents a perfectly fitting polynomial functions for the curve plotted in Fig. 3, then one should expect the difference $x - x_1$ is a constant, where x is the plotted curve in Fig. 3. Similarly, if x_2 represents a perfectly fitting polynomial functions for the curve plotted in Fig. 5, then one expects the difference $x - x_2$ is a constant, assuming x now is the plotted curve in Fig. 5. Contrarily, if $x - x_1$ (or $x - x_2$) is not a constant, then the polynomial x_1 (or x_2) cannot be a perfectly fitting polynomial function for the curve plotted in Fig. 3 (or Fig. 5).

Figure 7: Plot of $x - x_1$ for the case where $n_\phi = 1$ and $n_\theta = 1.5311$.Figure 8: Plot of $x - x_2$ for the case where $n_\phi = 1.5311$ and $n_\theta = 1$.

The results are shown in Figs. 7 and 8 respectively for the cases where $n_\theta > n_\phi$ and $n_\theta < n_\phi$. It clearly shows that $x - x_1$ or $x - x_2$ are far from being constants. This indicates that the surface cross-sectional profile of lens is not a simple parabolic curve as deceptively portrayed Fig. 3 (or Fig. 5). Instead, the magnification of the surface reveals series of kinked segments which must be attributed to the discrete continuous curve segments in instantaneous focal length (β) versus the lens radius (y) data shown in Fig. 1.

IV. CONCLUDING REMARKS

At the heart of software assisted image focusing technology is the specialized image reconstruction algorithm, which is permanently coded into the built in digital signal processor. The algorithm is often codified basing on the instantaneous focal length versus the lens radius data as the initial input. The software assisted image focusing

system therefore requires a specially designed lens whose output generates the instantaneous focal length versus the lens radius data. In this work, a formula for the lens surface profile has been presented. The derived lens formula generates a unique surface profile for the lens based on the instantaneous focal length versus the lens radius data. The lens design based on instantaneous focal length versus the lens radius data makes this result well suited for software assisted image focusing technology.

V. ACKNOWLEDGMENTS

I would like to thank G. Alexander and A. Lukyanov for providing the raw data for their instantaneous focal

length versus the lens radius profile described in their patent. I would also like to thank Dr. Seungwan Lee for the verification of the result using CODE V®[7] optical simulation tool. The author acknowledges the support for this work provided by Samsung Electronics, Ltd.

-
- [1] G. Alexander and A. Lukyanov, "Lens with extended depth of focus and optical system having the same," Korean Patent P2008-0043428 (2008).
 - [2] V. Portney, "Multifocal Ophthalmic Lens," U.S. Patent 4898461 (1990).
 - [3] S. Bradburn, W. Cathey, E. Dowski, "Realization of focus invariance in optical-digital systems with wave-front coding," *Appl. Opt.* **36** (35), pp. 9157-9166 (1997)
 - [4] E. Dowski, Jr., and W. Cathey, "Extended depth of field through wave-front coding," *Appl. Opt.* **34** (11), pp. 1859-1866 (1995)
 - [5] B. Forster, D. Van De Ville, J. Berent, D. Sage, and M. Unser, "Extended Depth-of-Focus for Multi-Channel Microscopy Images: A Complex Wavelet Approach," in *Proceedings of the Second IEEE International Symposium on Biomedical Imaging: From Nano to Macro (ISBI'04)*, (Arlington VA, USA, April 15-18, 2004), pp. 660-663.
 - [6] W. Derrick and S. Grossman, *A First Course in Differential Equations with Applications* (West Publishing Company, St. Paul, 1987).
 - [7] CODE V® is an optical design program with graphical user interface for image forming and fiber optical systems by Optical Research Associates (ORA), an organization that has been supporting customer success for over 40 years (www.opticalres.com).